

Modulation frequency and orientation tuning of second-order texture mechanisms

A. Serge Arsenault and Frances Wilkinson

Department of Psychology, McGill University, Montreal, Quebec, H3A 1B1, Canada

Frederick A. A. Kingdom

McGill Vision Research Unit, Department of Ophthalmology, McGill University, Montreal, Quebec, H3A 1A1, Canada

Received June 24, 1998; accepted September 21, 1998; revised manuscript received October 15, 1998

Modulation frequency and orientation tuning of second-order mechanisms underlying the detection of modulation in local spatial-frequency information are assessed by using an oblique-masking paradigm. Stimuli were Gabor-filtered noise patterns in which the local carrier spatial frequency was modulated about an average value of 4.7 cycles per degree (cpd) according to a sinusoidal function. Thresholds were determined for spatial-frequency modulated test patterns (0.2 and 0.8 cpd) with fixed vertical carrier and modulation orientations presented alone and in the presence of spatiotemporally superimposed masks. Mask modulation frequency (0.1, 0.2, 0.4, 0.8, or 1.6 cpd), modulation orientation (0°, 45°, or 90° relative to vertical), and carrier orientation (18.5° or 90° relative to vertical) were manipulated independently while the mask modulation amplitude remained fixed at 0.25. Manipulating the modulation frequency of the mask revealed some modulation frequency specificity, particularly at lower test modulation frequencies. Spatial-frequency modulated masks produced threshold elevations regardless of the local carrier orientation. However, there was no evidence of threshold elevation when the mask modulation orientation was orthogonal to that of the test pattern. These results suggest a second-order texture mechanism that is tuned to both modulation frequency and modulation orientation but is not selective in terms of the orientation of first-order inputs. © 1999 Optical Society of America [S0740-3232(99)02403-5]

OCIS codes: 330.7310, 330.5510, 330.1880.

1. INTRODUCTION

Much is known about mechanisms that encode the local spatial structure found in visual texture. However, research is only beginning to reveal the properties of mechanisms that integrate this local information across space, giving rise to the more global phenomenon that is texture. In the present study, we examine the spatial properties of mechanisms underlying the detection of gradients in local spatial-frequency information. Such mechanisms are likely to be implicated in the encoding of shape from texture.

Results from studies on the effectiveness of texture cues to surface shape indicate that compression is the most salient cue.¹⁻³ Compression gradients can be defined as changes in local spatial-frequency information produced by variations in surface shape that are confined to orientations perpendicular to the direction of variation in surface shape. In the case of discrete micropattern textures, the salience of texture compression is not reducible to changes in the aspect ratio of the micropatterns.² In addition, the significance of compression appears to depend on the composition of the surface texture. Those textures that, under the influence of compression, contain a systematic change in local peak spatial frequency produce the most striking impression of surface depth.⁴ Such textures have also been shown to produce lower detection thresholds than textures that do not contain sys-

tematic changes in local peak spatial frequency, as is the case, for example, when texture density is modulated.⁵

The issue of how compression information is encoded to extract direction and magnitude of depth has been addressed in the modeling work of Sakai and Finkel.⁴ In the final stages of their model, they propose an algorithmic solution to the problem of integrating compression information across space. In their model nominal peak spatial-frequency values characterizing the information contained at different points on the surface are integrated along the steepest gradient, starting at the lowest value. This is done independently for information at four orientations. The integration provides an estimate of depth, and the orientation for which it was calculated gives the direction of modulation in depth. The question remains as to how this algorithm might be implemented in the visual system.

The purpose of this study is to characterize the mechanisms involved in the detection of second-order spatial-frequency information (i.e., gradients in local spatial frequency), mechanisms that may be involved in the perception of surface shape based on gradients in texture compression. An oblique-masking technique^{6,7} is used to assess the orientation tuning and the spatial-frequency selectivity of these second-order mechanisms. Bowen and Wilson⁷ have successfully applied this technique in their analysis of pattern masking. They measured

thresholds for detecting narrow-band spatial-frequency stimuli in the presence of various masks. By comparing the effects of uniform-luminance field masks of different polarity and cosine grating masks, they were able to dissociate masking effects that are due to pointwise luminance adaption (early masking process) from those stemming from spatial-frequency and orientation-tuned filters (late masking process).

Following the same logic, we seek to isolate the contribution of second-order spatial-frequency mechanisms from that of first-order spatial-frequency mechanisms and subsequently determine some of the properties of the second-order mechanisms. In experiment 1 we assess the spatial-frequency selectivity of second-order texture mechanisms by comparing the masking effects of spatial-frequency modulated masks (second order) of various modulation frequencies with those of unmodulated masks (first order only). In experiment 2 the orientation tuning of second-order mechanisms is assessed in terms of both the first-order inputs and the second-order modulation orientation. Selectivity for first-order oriented inputs is determined by comparing masking effects of spatial-frequency modulated and unmodulated masks having different first-order carrier orientations. Second-order orientation tuning is determined by comparing the masking effects of spatial-frequency modulated masks of different modulation orientations with those of unmodulated masks.

2. METHODS

A. Subjects

Three subjects with normal or corrected-to-normal vision participated in the experiment. Subjects SA (one of the authors) and AL were not naive as to the purposes of the study.

B. Stimulus Generation and Display

The stimuli ($15.08^\circ \times 15.08^\circ$) were spatial-frequency modulated texture patterns produced by combining filtered noise patterns that varied in their spatial-frequency content (Fig. 1). A basis set of three filtered noise patterns was used to produce sinusoidally modulated patterns of a given modulation amplitude. Each base pattern was obtained by convolving an oriented Gabor filter with a uniform random-noise pattern. For all stimuli one of the base patterns represented average spatial-frequency information and was produced with a circular Gabor filter having a carrier wavelength of 0.21° [4.7 cycles per degree (cpd)] and a space constant of 0.20° . The space constant is defined as the distance from the center of the filter at which the envelope amplitude is equal to $1/e$. Therefore the full-octave bandwidth of the filter at half-height was 0.8. The remaining two base patterns represented spatial-frequency information at the extremes of the modulated function, and thus their spatial-frequency content was dependent on the modulation amplitude. These patterns were obtained by scaling the filter along the dimension perpendicular to its carrier orientation. This was accomplished by varying the carrier wavelength and the space constant proportionally about their respective average values by a factor determined by the modulation amplitude. Spatial-frequency modulated texture patterns were subsequently created by combining the three base patterns according to the following formulas:

$$T_{FM}(x, y) = \begin{cases} B_L(x, y)M(x, y) + B_A[1 - |M(x, y)|], & M(x, y) > 0 \\ B_H(x, y)M(x, y) + B_A[1 - |M(x, y)|], & M(x, y) < 0 \\ B_A(x, y), & M(x, y) = 0 \end{cases} \quad (1)$$

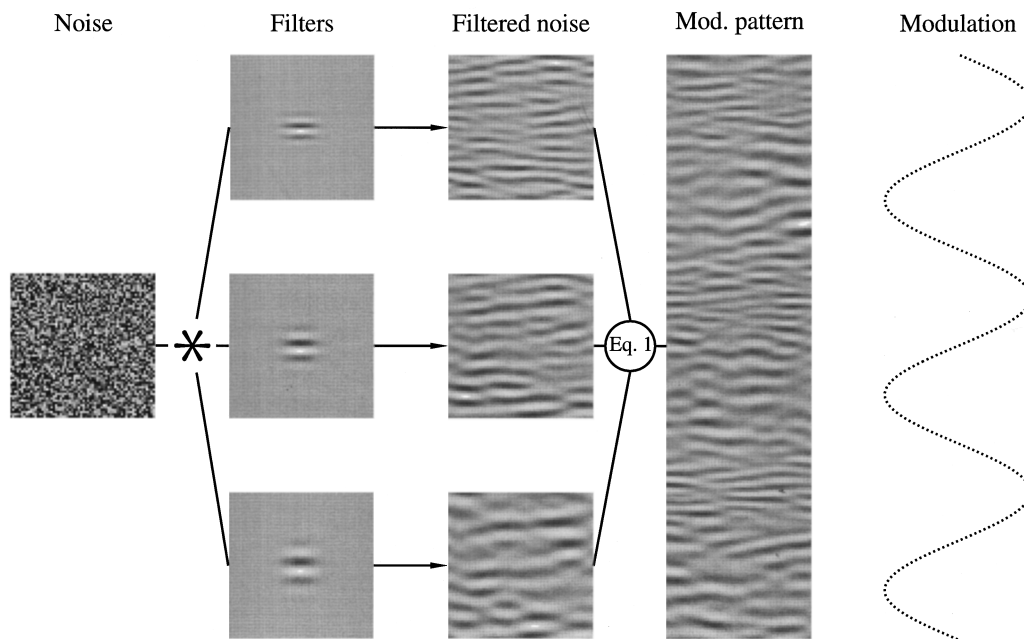


Fig. 1. Schematic representation of the stimulus generation process. Filtered noise patterns are generated by convolving Gabor filters having different spatial properties with a uniform random-noise pattern. The filtered noise patterns are subsequently combined according to Eq. (1) to produce a spatial-frequency modulated texture pattern. The function at the bottom of the figure represents the modulation portrayed in the modulated pattern.

where B_L , B_H , and B_A are the low, high, and average spatial-frequency base patterns. The modulation function, represented by M , was sinusoidal and had values ranging from -1 to 1 . The luminance contrast of the final pattern was set to 0.5 . An example of a spatial-frequency modulated pattern is shown in Fig. 2A.

The technique is analogous to that used to generate red/green luminance gratings, except that in our case local spatial frequency is modulated rather than color and three rather than two basis patterns are used. The resulting patterns are an approximation of the effects produced by the sinusoidal modulation of texture compression gradients. When modulation amplitudes are too high, the spatial-frequency distribution becomes trimodal, which would not be the case in an actual smoothly varying surface. However, given that we are measuring detection thresholds, approximations generated from a three-pattern basis set should be adequate for the range of modulation amplitudes studied. The benefit of this technique over others^{8,9} for generating pattern-modulated band-limited noise textures is its computational efficiency.

Both test and mask patterns were generated as described above. The test pattern carrier and modulation orientations were vertical throughout the experiments presented in this paper, whereas the mask carrier and modulation orientations varied depending on the condition. The modulation frequency of both the test and the mask was also manipulated. Masked patterns were produced by adding test and mask luminances such that the average luminance remained constant at 50 cd/m^2 . Given a luminance contrast of 0.5 for each pattern, the theoretical maximum luminance contrast of the masked pattern was 1 (Fig. 2C).

Stimuli were displayed on a Macintosh 19-in. monitor driven by a PowerMac 7100 computer with the use of a video card with 8-bit (256 gray levels) intensity resolution. Following calibration with a Hagner spot photometer, 140 of the initial 256 levels were retained to form a z -linearized lookup table. Stimuli were displayed at a vertical refresh rate of 75 Hz by using lookup-table animation techniques. All stimuli were viewed binocularly at a distance of 57 cm in a dimly lit room.

C. Procedure

A two-alternative temporal forced-choice paradigm with the method of constant stimuli was used to determine spatial-frequency modulation thresholds. A typical trial began with the presentation of a fixation cross ($18' \times 18'$) in the center of the display. Following a subject-initiated space-bar press, two stimulus intervals of 240 ms each were presented, separated by a 750-ms blank interval during which the entire screen was set to the mean luminance level of a given texture pattern or 50 cd/m^2 . One stimulus interval contained a spatial-frequency modulated test pattern (with or without mask), and the other contained an unmodulated test pattern (with or without mask). The subject's task, whether masks were present or not, was to indicate which interval contained the modulated test pattern by pressing one of two computer keys. Five test modulation amplitudes were used in determining each threshold.

D. Data Analysis

Psychometric data for each run were fitted with a Quick function by using a Levenberg–Marquardt least-squares procedure. Thresholds were defined as the sinusoidal modulation amplitude associated with 75% detection accuracy. Reported thresholds are the thresholds averaged across the three runs.

Masking effects are presented as threshold shifts and have the following general form:

$$\Delta \text{th} = \frac{\text{th}_{\text{masked}}}{\text{th}_{\text{baseline}}}, \quad (2)$$

where $\text{th}_{\text{masked}}$ is the threshold containing the masking effect of interest and $\text{th}_{\text{baseline}}$ is the threshold containing effects to be factored out. For example, the contribution of the second-order modulation to the overall masking effect is determined by factoring out first-order local masking effects. This would entail taking the ratio of modulated to unmodulated mask condition thresholds.

3. EXPERIMENT 1

The purpose of this experiment was to determine basic sensitivity to spatial-frequency modulated patterns and to assess the modulation frequency selectivity of second-order texture mechanisms. We first measured spatial-frequency modulation thresholds for test patterns presented alone (unmasked thresholds). Thresholds were obtained for two modulation frequencies (0.2 and 0.8 cpd). Subjects completed three experimental sessions of two runs each, one for each modulation frequency. A given run consisted of 30 trials per condition or 150 trials ($30 \text{ trials} \times 5 \text{ modulation amplitudes}$).

Thresholds were then determined for spatial-frequency modulated test patterns in the presence of masks. Spatial-frequency modulated and unmodulated masks were used to assess second-order and first-order masking effects, respectively. For modulated masks, modulation frequencies spanning a total range of approximately four octaves (0.1 , 0.2 , 0.4 , 0.8 , and 1.6 cpd) were tested with a fixed modulation amplitude of 0.25 . The mask carrier orientation was vertical, and the modulation orientation was 18.5° , an offset that allowed for all possible modulation phase relationships between test and mask to be represented within the same stimulus (Fig. 2B). Three runs were completed for each mask condition, with a given run consisting of 30 trials per test modulation amplitude.

A. Unmasked Thresholds

Thresholds for spatial-frequency modulated test patterns presented alone are plotted as a function of modulation frequency in Fig. 3. Subjects are quite sensitive to sinusoidal modulation of local spatial-frequency information, with average threshold of 0.06 . These findings corroborate our earlier work with discrete micropattern textures.⁵ In addition, thresholds are quite consistent across subjects and conditions (standard deviation = 0.01) with one exception, subject CB's results at 0.8 cpd .

Based on these findings, it is not possible to determine whether the sensitivities described are the result of a single mechanism or multiple modulation-frequency-

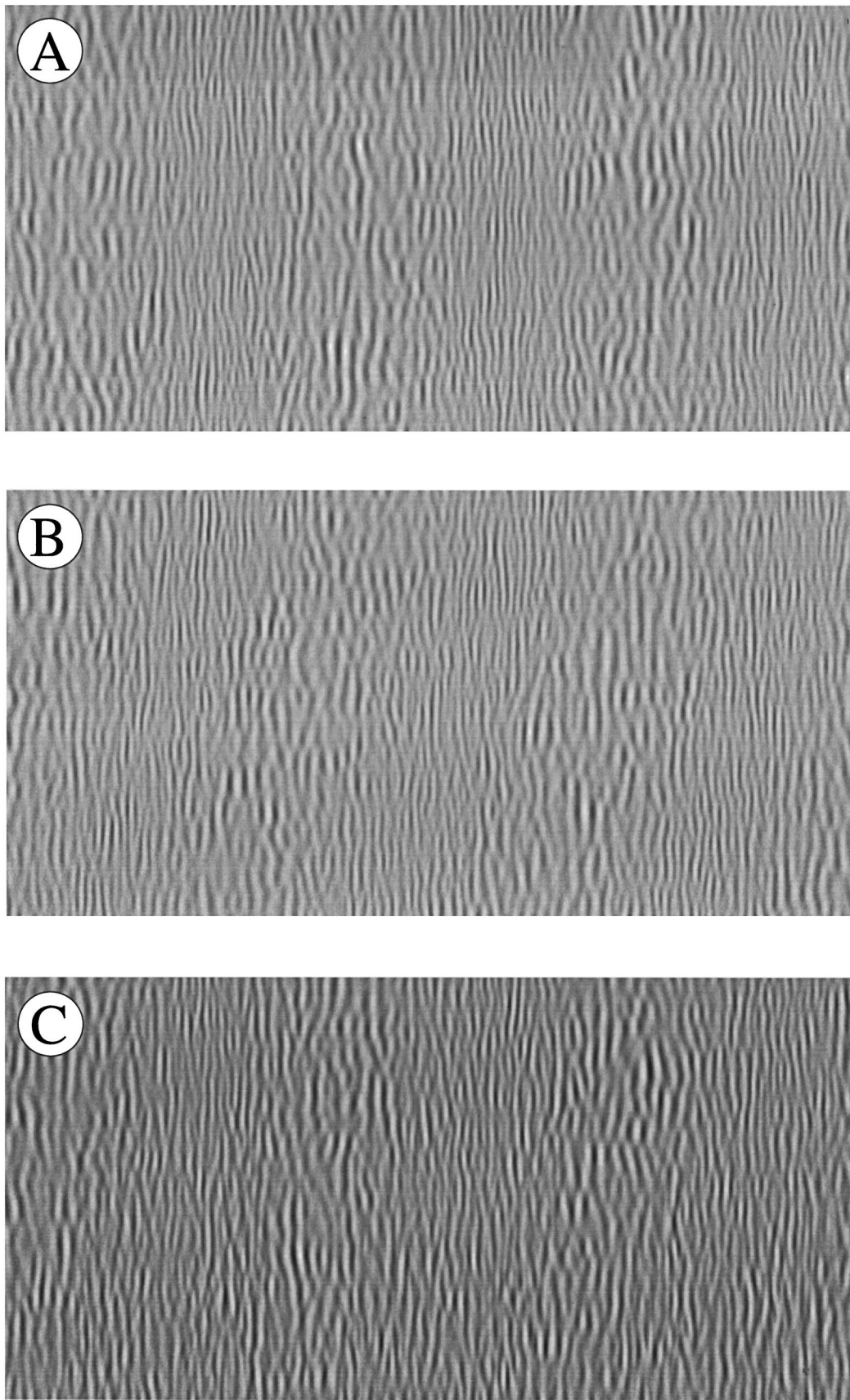


Fig. 2. Example stimuli. A, Spatial-frequency modulated test pattern depicting three cycles of modulation at a modulation amplitude of 0.25. B, Spatial-frequency modulated mask pattern with a modulation orientation of 18.5° relative to vertical and a modulation amplitude and frequency similar to those of the test pattern in A. C, Combination of the test and mask patterns described in A and B. The actual patterns used in the experiment were double the heights of those depicted here.

selective mechanisms. The results presented in Subsection 3.B address this issue directly.

B. Second-Order Modulation Frequency Selectivity

In this phase of the experiment, mask modulation frequencies were manipulated to assess the modulation frequency selectivity of second-order texture mechanisms. Threshold shifts are plotted as a function of mask modulation frequency for each test modulation frequency in Fig. 4. Threshold shifts represent the ratio of modulated to unmodulated mask condition thresholds. A value above 1 indicates a contribution of the modulation to the masking effect (second-order masking effect), whereas a value equal to 1 suggests no contribution of the modulation. First, there is a clear second-order masking effect. All subjects show conditions under which threshold shifts are above 1. In the case of subject SA for the 0.2-cpd test and the 0.2-cpd mask, there is almost a twofold increase in threshold when the mask is modulated relative to when it is not. Second, there is evidence of modulation frequency selectivity in the 0.2-cpd test pattern condition. All subjects show a clear peak where masking is optimal, with the effect weakening as modulation frequency increases or decreases from this point. Precisely where

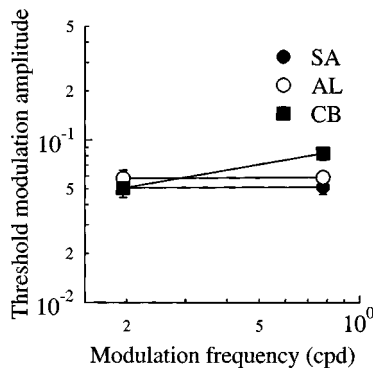


Fig. 3. Unmasked thresholds for spatial-frequency modulated test patterns plotted as a function of modulation frequency.

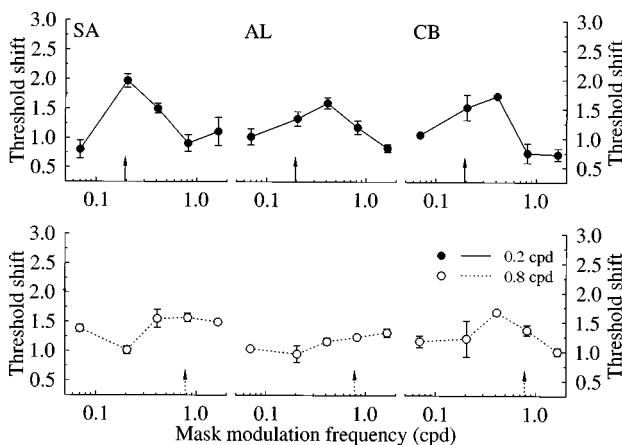


Fig. 4. Modulation-frequency-specific masking effects. Threshold shift is plotted as a function of mask modulation frequency for two test pattern modulation frequencies. Threshold shifts represent modulated mask thresholds normalized with unmodulated mask thresholds. The vertical arrows along the abscissa correspond to the test pattern modulation frequencies.

Table 1. Estimated Peak Frequency and Bandwidth of Second-Order Mechanisms

Subject	Peak (cpd)	Bandwidth ^a
SA	0.24	1.45
AL	0.36	1.74
CB	0.31	1.43

^a Full width at half-height in octaves.

this peak occurs varies across subjects but is limited to one of two values: either the mask modulation frequency most similar to that of the test or the next highest mask modulation frequency. To provide a more quantitative description of the properties of the underlying mechanism, the data in question were fitted with a function of the following form:

$$y = 1 + a \exp[-(x - f_0)^2/s^2], \quad (3)$$

where a is the amplitude of the function, f_0 is the peak modulation frequency, and s is the space constant. The amplitude parameter was always fixed at $1 - ts_{\max}$, where ts_{\max} is the largest threshold shift in the dataset to be fitted. Estimated peak modulation frequencies and bandwidths are presented in Table 1.

Results for the 0.8-cpd test modulation frequency are not as consistent across subjects. However, threshold shifts for the 0.8-cpd test pattern are noticeably larger than those obtained with the 0.2-cpd test pattern for the two highest modulation frequency masks, suggesting the involvement of distinct second-order mechanisms.

4. EXPERIMENT 2

The purpose of this experiment was to explore the orientation tuning properties of second-order texture mechanisms. Orientation tuning was assessed both in terms of first-order inputs (i.e., the orientation of local luminance information) and in terms of the orientation of the second-order spatial-frequency modulation.

The three subjects from experiment 1 and a new subject, FW, participated in this experiment. Stimuli were generated as described in Subsection 2.B, except that in one condition the mask carrier orientation was varied (0° , 45° , or 90°) while the modulation orientation remained fixed at 18.5° . In another condition the mask modulation orientation was varied (18.5° or 90°) while the carrier orientation was constant at 0° . These manipulations were designed to assess first- and second-order orientation tuning properties, respectively. Only the 0.2-cpd test pattern condition was tested and only with a mask modulation frequency of 0.2 cpd. It is important to remember that a given basis set was generated by manipulating the carrier wavelength and the space constant perpendicular to the carrier orientation. This ensures that patterns differing in carrier orientation differ only in orientation and not in spatial-frequency content. Examples of mask patterns from the two conditions are presented in Fig. 5, one having a horizontal carrier orientation and the other having a horizontal modulation orientation.

A. First-Order Orientation Tuning

To assess the first-order orientation tuning properties of second-order mechanisms, thresholds obtained with modulated and unmodulated masks were transformed into threshold shifts by normalizing these values with standard threshold values (i.e., without a mask), as obtained in experiment 1. Figure 6 presents threshold shifts plotted as a function of mask carrier orientation for both modulated and unmodulated masks.

Under both masking conditions, threshold shifts increase as the mask carrier orientation approaches that of the test. For the unmodulated mask condition, horizontal mask carriers produced threshold shift values near 1, with a mean elevation of 1.11, suggesting the lack of a masking effect. At mask carrier orientations of 45° , there is little change ($\bar{x} = 1.27$), followed by a more substantial increase when mask and test carrier orientations are identical ($\bar{x} = 1.94$). Threshold shifts are larger

with the modulated mask but exhibit a similar trend, with mean threshold elevations of 1.75, 1.70, and 2.61 for horizontal, oblique, and vertical mask carriers, respectively.

Results for the unmodulated mask condition are analogous to findings from studies on orientation tuning with masking.¹⁰ As expected, the greatest masking effects occur when the mask carrier orientation matches that of the test pattern. In fact, there was little if any masking effect with unmodulated orthogonal carrier masks. What is striking, however, is that adding spatial-frequency modulation to an orthogonal carrier mask produces a significant masking effect, which suggests that second-order texture mechanisms receive inputs from both similarly oriented and orthogonally oriented first-order units.

To assess whether the masking obtained with modulated orthogonal carrier masks stems from mechanisms similar to those involved when mask and test have iden-

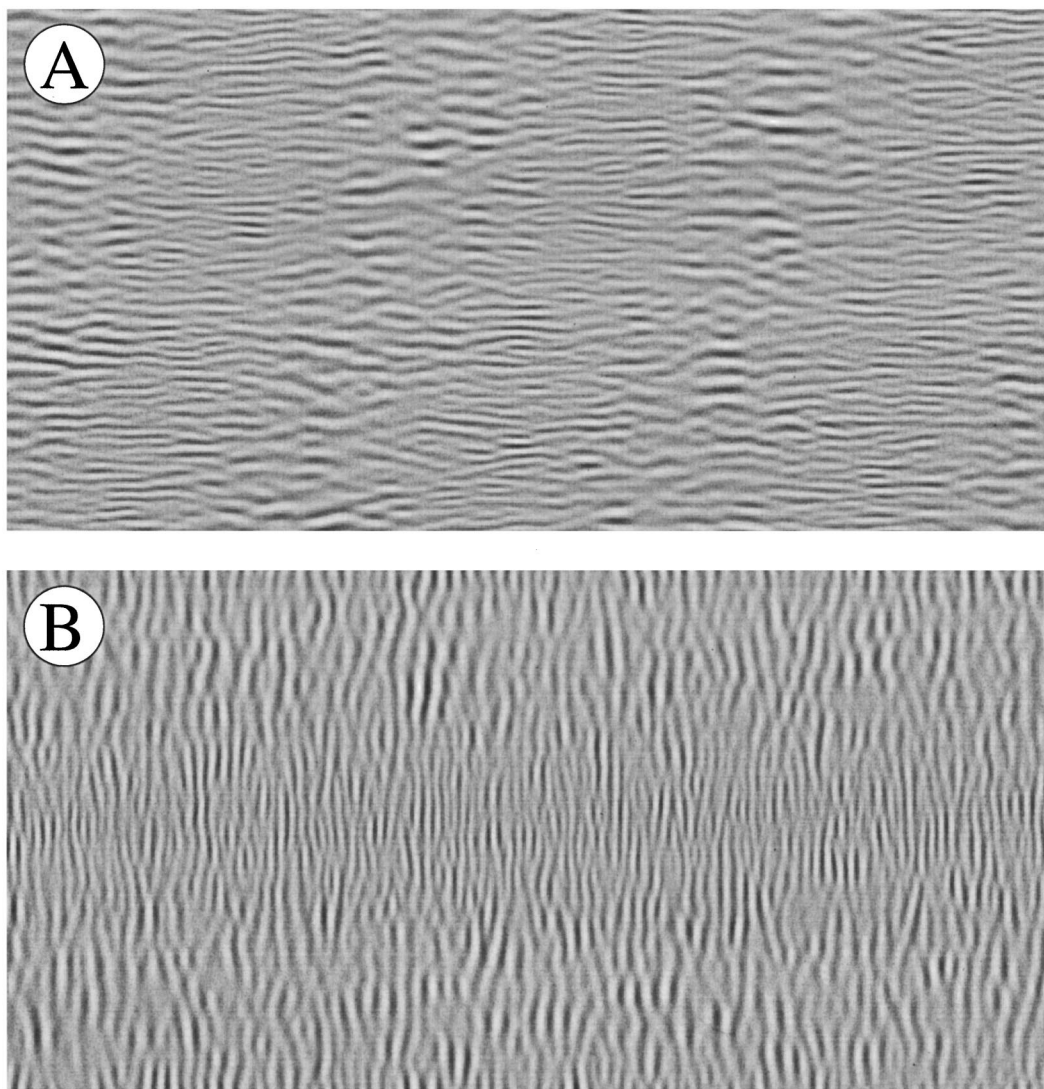


Fig. 5. Example mask patterns used to assess the orientation tuning of second-order texture mechanisms. A, Spatial-frequency modulated mask pattern with horizontal carrier. The pattern depicts three cycles with a modulation orientation of 18.5° relative to vertical and a modulation amplitude of 0.25. This mask was used to assess first-order orientation tuning properties of the second-order mechanism. B, Horizontal modulation orientation mask depicting similar modulation frequency and amplitude to those in the pattern in A but with vertical carrier. This mask was used to assess second-order orientation tuning properties. The actual mask patterns used in the experiment were double the heights of those depicted here.

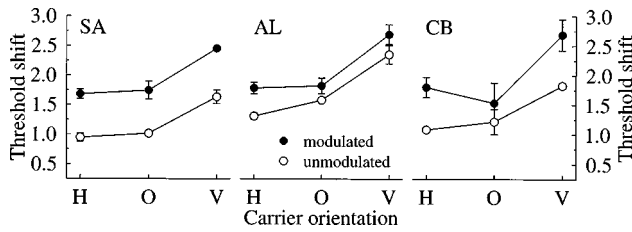


Fig. 6. First-order carrier-orientation-specific masking effects. Threshold shift is plotted as a function of mask carrier orientation (H = horizontal, O = oblique, V = vertical). Threshold shifts represent either modulated mask thresholds (filled circles) or unmodulated mask thresholds (open circles) normalized with base thresholds as depicted in Fig. 3. The test pattern had a vertical carrier and a vertically oriented modulation of 0.2 cpd.

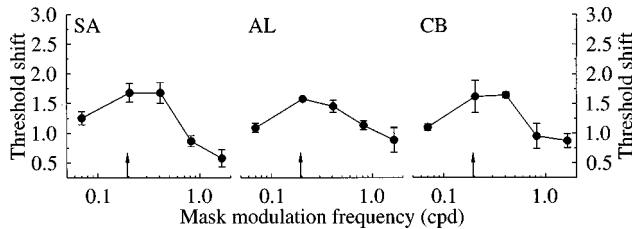


Fig. 7. Second-order modulation-frequency-specific masking effects for masks with orthogonal carriers. Threshold shift is plotted as a function of mask modulation frequency for a 0.2-cpd test pattern. Threshold shifts represent modulated mask thresholds normalized with unmodulated mask thresholds. The vertical arrows along the abscissa correspond to the test pattern modulation frequency.

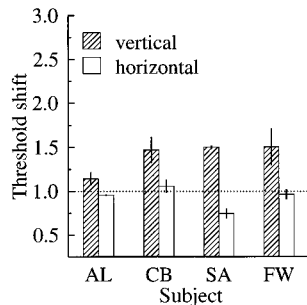


Fig. 8. Second-order orientation-specific masking effects. Threshold shift is plotted for each subject for two different mask modulation orientations (18.5° and 90° relative to vertical). Threshold shifts were calculated by normalizing modulated mask thresholds with the unmodulated mask threshold. The dotted line represents the case where the modulation does not contribute to the masking effect, and therefore the overall masking effect can be accounted for by first-order masking effects. The test pattern had a vertical carrier and a vertically oriented modulation of 0.2 cpd.

tical carrier orientations, we repeated experiment 1 by using masks with horizontal carriers. Thresholds were measured for the 0.2-cpd test pattern masked with modulated orthogonal carrier masks of various modulation frequencies and a fixed modulation orientation of 18.5° . The results, plotted in Fig. 7, demonstrate the same qualitative trend as that when the carrier orientation of the modulated mask is identical to that of the test. For both mask carrier orientations, we obtain peak masking effectiveness at mask modulation frequencies near or

identical to the modulation frequency of the test pattern. This implies the existence of spatial-frequency modulation encoding mechanisms with different carrier orientation tuning.

B. Second-Order Orientation Tuning

To test for second-order orientation tuning, vertical modulation test patterns were masked with patterns having a modulation orientation of either 18.5° or 90° relative to vertical and a vertical carrier. Results are expressed as threshold shifts in Fig. 8, where threshold shifts represent the ratio of modulated to unmodulated mask condition thresholds. A threshold shift of 1 would indicate no second-order masking effect. In all cases threshold shifts were largest when the orientation of the mask modulation was similar to that of the test pattern. The mean threshold shift for this condition was 1.41, indicating a clear contribution from the modulation. On the other hand, a mean threshold shift of 0.93 for the orthogonal modulation orientation mask suggests no contribution of the modulation. Three of the four subjects (AL, CB, and FW) had threshold shift values near 1. However, for subject SA, the threshold shift was far enough below 1 to suggest some form of facilitation. The results are consistent with a second-order mechanism that is tuned for the orientation of the spatial-frequency modulation.

5. GENERAL DISCUSSION

Our results show that the visual system is quite sensitive to modulation of local spatial-frequency information and that this sensitivity is relatively constant for the two test modulation frequencies studied. Similar results have been found for the detection of frequency-modulated (FM) gratings, stimuli that share some characteristics with those studied in the present experiment. Studies on FM grating detection^{11,12} report thresholds that are quite low but not as low as those found in our experiment, which averaged to 0.06. Under comparable conditions FM thresholds ranged from 0.08 to 0.11, with little change as a function of modulation frequency. The fact that our thresholds differ from FM thresholds may be related to differences in the composition of the stimuli used. FM gratings contain a fundamental spatial-frequency component at the carrier frequency and sideband components at multiples of the modulation frequency relative to the carrier. The energy associated with these sideband components decreases with distance from the carrier frequency. Detection of FM gratings is thought to be dependent on the detection of these spatial-frequency sidebands.^{11,12} Our stimuli differ from these in the sense that they do not contain discrete sidebands. The amplitude spectrum of one of our spatial-frequency modulated patterns is a combination of the spectra of the three basis patterns. For the range of modulation amplitudes used in the present experiment, this produces a relatively full distribution of components rather than isolated components occurring with a certain periodicity, as is the case with FM gratings.

A potential explanation for both FM grating thresholds and our spatial-frequency modulation thresholds can be found in the work on spatial-frequency discrimination.

Psychophysical estimates of spatial-frequency discrimination thresholds range from 3% to 9%.¹³⁻¹⁶ Thresholds of this order could be accounted for by the differential response of a single spatial-frequency channel. In fact, spatial-frequency-tuned neurons in cat visual cortex have been shown to produce reliably distinct responses to spatial-frequency differences of 5%.¹⁷ To compare these results with ours, it is important to note that the maximum difference in spatial frequency depicted in one of our stimuli is in fact twice the modulation amplitude. When this is taken into account, our thresholds are roughly twice those typically found in spatial-frequency discrimination experiments. The average modulation amplitude threshold was 0.06, producing a total change in spatial frequency of 12%. It is difficult to estimate how much of this discrepancy in threshold might be due to the higher noise content and the wider bandwidth of our stimuli as compared with those of cosine gratings. However, it is clear that the thresholds that we report, as well as those reported for FM gratings, fall well within the range of differences in spatial frequency discriminable by single spatial-frequency channels.

A model based on the differential responses of a single spatial-frequency channel provides an adequate explanation of our unmasked threshold results. However, our findings in experiment 1 showing modulation frequency tuning require additional considerations. These findings imply that the underlying mechanism is sensitive not only to the absolute change in local spatial frequency but also to the rate of change in spatial frequency. To account for these results, one might propose a mechanism similar to the one depicted schematically in Fig. 9A. First-order units with properties analogous to those of simple cells begin by characterizing the local spatial structure of the pattern. Following rectification of their responses, first-order units of a given spatial frequency and orientation channel within a restricted local neighborhood feed into a second-order unit. In this model the orientations of the first- and second-order units are matched. The second-order unit then pools the responses of the first-order units according to a spatial weighting function, which in our case is a two-dimensional Gabor. Excitatory and inhibitory regions of the receptive field of the second-order mechanism are balanced such that an unmodulated pattern would produce no response in this unit. The characteristics of this weighting function could be varied, allowing one to define second-order mechanisms with different modulation frequency and modulation orientation selectivities.

Our manipulations involving the carrier orientation of the mask clearly distinguished the properties of the first-order mechanisms from those of the second-order mechanisms. Unmodulated mask patterns produced an orientation-dependent effect, a result consistent with the orientation tuning properties of first-order mechanisms.¹⁰ Modulated masks produced a similar trend but with greater threshold shifts than those obtained with unmodulated masks, regardless of the carrier orientation. By factoring out the first-order effects (e.g., by taking the ratio of modulated to unmodulated mask thresholds), we see that the second-order effect is largely first-order orientation nonspecific.

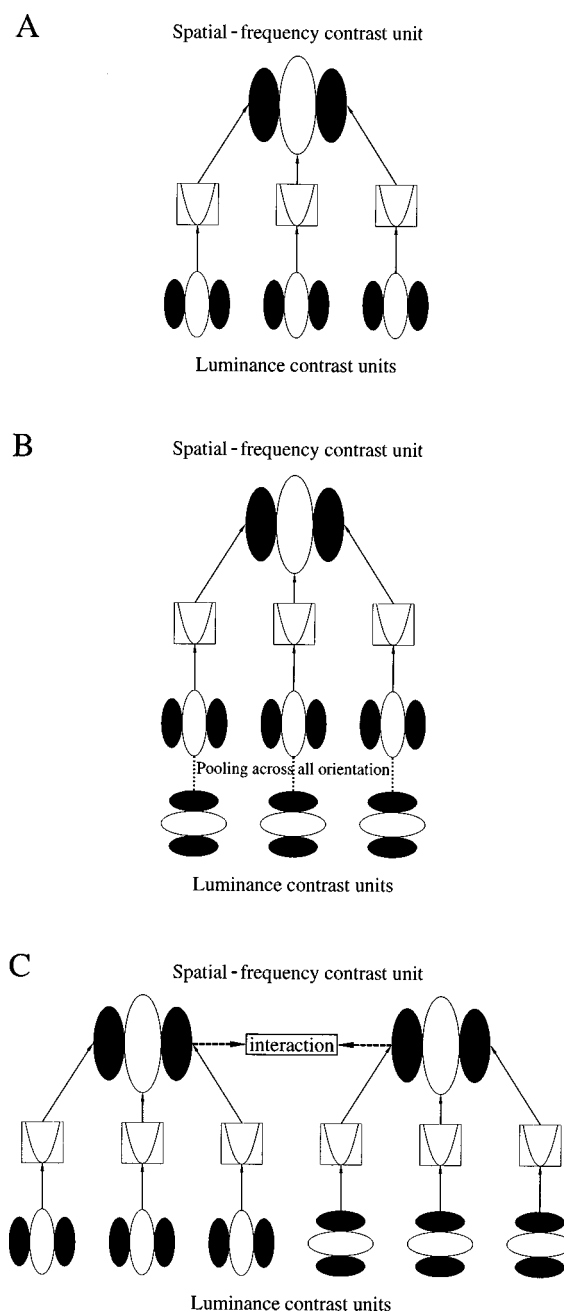


Fig. 9. Schematic representations of three different second-order texture mechanisms. A, The responses of first-order luminance contrast encoding units with identical spatial-frequency and orientation selectivities are full-wave rectified and subsequently feed into a second-order unit with similar orientation tuning properties. The spatial weighting function applied to the outputs of the first-order units allows the second-order unit to encode gradients in local spatial-frequency information. B, Mechanism similar to the one in A, except that first-order inputs are pooled across all orientations following the rectification process. C, Model incorporating interaction between second-order units with different first-order oriented inputs. This interaction could be in the form of direct inhibition between second-order units or pooling of second-order responses in a higher-level mechanism.

Accounting for these results requires revising the basic mechanism described above (Fig. 9A). One possible modification to the basic model would be to have the second-order mechanism pool across all orientations.

This model is represented schematically in Fig. 9B. The outputs of first-order mechanisms representing all orientations are pooled by taking a weighted sum for each spatial location. This integration of responses across all orientations would effectively produce masking for modulated masks with orthogonal carriers. However, it would also predict a significant masking effect for unmodulated masks with orthogonal carriers. This was not found, as evidenced by the results shown in Fig. 6.

The model depicted in Fig. 9C corrects the shortcomings of the previous model. The logic of the basic mechanism is extended to include second-order mechanisms that receive as input the responses of first-order units at orthogonal orientations. The second-order units then interact either through a direct inhibitory connection or through the pooling of their outputs in a higher-level mechanism. In this scenario an unmodulated orthogonal carrier mask pattern would not activate either of the two second-order mechanisms; activation of second-order units occurs only in the presence of local spatial-frequency modulation. Detection of the test pattern would thus be unaffected by the presence of this particular mask. A modulated orthogonal carrier mask would activate the second-order unit receiving input from orthogonal first-order units. Because of the interaction between second-order units, this mask would produce significant masking of the test pattern. This type of interaction between mechanisms that represent spatial-frequency gradients at different orientations has been proposed by Sakai and Finkel⁴ in the form of cross-orientation inhibition to account, in part, for the poor performance of perspective scaling in determining shape from texture. Although implemented in a different manner here, it could serve essentially the same purpose.

Finally, our results showing no masking effect with orthogonal modulation orientation masks suggest that the second-order mechanism is orientation selective for the modulation. This supports our choice of oriented filters to represent second-order units.

6. CONCLUSION

We have attempted to elucidate some of the spatial properties of mechanisms involved in the detection of gradients in local spatial-frequency information. The results suggest a mechanism that is tuned for both modulation frequency and modulation orientation. In addition, it is orientation selective in terms of its first-order inputs but appears to be affected by modulation of local spatial-frequency information in any orientation. Further research should concentrate on a finer characterization of the tuning properties of these second-order units and establishing more clearly the relationship between first- and second-order spatial-frequency properties.

ACKNOWLEDGMENTS

This research was supported by Natural Sciences and Engineering Research Council grant OGP0007551 given to F. Wilkinson and Natural Sciences and Engineering Research Council Grant OGP0121713 given to F. A. A. Kingdom.

Address correspondence to A. Serge Arsenault at the location on the title page or e-mail, serge@ego.psych.mcgill.ca.

REFERENCES

1. J. E. Cutting and R. T. Millard, "Three gradients and the perception of flat and curved surfaces," *J. Exp. Psychol.* **113**, 198–216 (1984).
2. J. T. Todd and R. A. Akerstrom, "Perception of three-dimensional form from patterns of optical texture," *J. Exp. Psychol.* **13**, 242–255 (1987).
3. A. Blake, H. H. Bülhoff, and D. Sheinberg, "Shape from texture: ideal observers and human psychophysics," *Vision Res.* **33**, 1723–1737 (1993).
4. K. Sakai and L. H. Finkel, "Characterization of the spatial-frequency spectrum in the perception of shape from texture," *J. Opt. Soc. Am. A* **12**, 1208–1224 (1995).
5. A. S. Arsenault, F. A. A. Kingdom, and F. Wilkinson, "Relative salience and interaction of texture cues to surface shape," *Perception* (to be published).
6. H. R. Wilson, D. K. McFarlane, and G. C. Phillips, "Spatial frequency tuning of orientation selective units estimated by oblique masking," *Vision Res.* **23**, 873–882 (1983).
7. R. W. Bowen and H. R. Wilson, "A two-process analysis of pattern masking," *Vision Res.* **34**, 645–657 (1994).
8. M. S. Landy and J. R. Bergen, "Texture segregation and orientation gradient," *Vision Res.* **31**, 679–691 (1991).
9. J. R. Bergen and M. S. Landy, "Computational modeling of visual texture segregation," in *Computational Models of Visual Processing*, M. S. Landy and J. A. Movshon, eds. (MIT Press, Cambridge, Mass., 1991), Chap. 10, pp. 253–271.
10. G. C. Phillips and H. R. Wilson, "Orientation bandwidths of spatial mechanisms measured by masking," *J. Opt. Soc. Am. A* **1**, 226–232 (1984).
11. J. H. T. Jamar, J. C. Campagne, and J. J. Koenderink, "Detectability of amplitude- and frequency-modulation of suprathreshold sine-wave gratings," *Vision Res.* **22**, 407–416 (1982).
12. J. H. T. Jamar, L. F. T. Kwakman, and J. J. Koenderink, "The sensitivity of the peripheral visual system to amplitude-modulation and frequency-modulation of sine-wave patterns," *Vision Res.* **24**, 243–249 (1984).
13. F. W. Campbell, J. Nachmias, and J. Jukes, "Spatial-frequency discrimination in human vision," *J. Opt. Soc. Am.* **60**, 555–559 (1970).
14. C. A. Burbeck and D. Regan, "Independence of orientation and size in spatial discriminations," *J. Opt. Soc. Am.* **73**, 1691–1694 (1983).
15. T. Caelli, H. Brettel, I. Rentschler, and R. Hinz, "Discrimination thresholds in the two-dimensional spatial frequency domain," *Vision Res.* **23**, 129–133 (1983).
16. R. Blake, K. Holopigian, and H. R. Wilson, "Spatial-frequency discrimination in cats," *J. Opt. Soc. Am. A* **3**, 1443–1449 (1986).
17. A. Bradley, B. C. Skottun, I. Ohzawa, G. Sclar, and R. D. Freeman, "Neurophysiological evaluation of the differential response model for orientation and spatial-frequency discrimination," *J. Opt. Soc. Am. A* **2**, 1607–1610 (1985).